J|A|C|S
ARTICLES
Published on Web 02/09/2007

Energy-Resolved Collision-Induced Dissociation Cross Sections of 2:1 Bis-oxazoline Copper Complexes. Nonbonded Interactions and Nonlinear Effects

Eva Zocher, Rolf Dietiker, and Peter Chen*

Contribution from the Laboratorium für Organische Chemie, ETH Zürich, Switzerland

Received July 27, 2006; E-mail: peter.chen@org.chem.ethz.ch

Abstract: Absolute ligand binding energies are determined for the 2:1 complexes of *bis*-oxazoline ligands and Cu(I) in the gas phase by the fitting of energy-resolved collision-induced dissociation cross sections. The complexes were chosen for their occurrence in asymmetric catalysis for which the phenomenon of nonlinear effects is explained by differences in stability for homochiral and heterochiral complexes. *Pseudo*-enantiomeric ligands are used so that mass spectrometric measurements can be employed. The measurements find that the sterically similar, but electronically different, isopropyl versus phenyl substituents lead to a different stability ordering of the homo- versus heterochiral complexes, which then leads to the prediction of nonlinear effects in asymmetric catalysis by the complexes with isopropyl-substituted ligands. The origin of the difference in stability order is found in noncovalent interactions between the phenyl groups on the ligands, which are poorly described by DFT calculations.

Introduction

Whereas small differences in the stability of diastereomeric metal−ligand complexes are routinely invoked to explain stereoselectivity in asymmetric catalysis, very few quantitative studies of their thermochemistry have been reported. Of particular interest in recent years are nonlinear effects. The phenonenon, first worked out by Kagan,[1] deals with the initially paradoxical observation that asymmetric catalysis with an enantiomerically impure chiral ligand can produce products whose optical purity, as measured by enantiomeric excess (ee), is higher than that of the ligand. Nonlinear effects have been shown for a wide range of catalytic reactions, including, for example, the Sharpless epoxidation[2] and diethyl zinc additions,[3] and many other important transformations. The phenomenon has been postulated as an explanation for the predominance of only one enantiomer of amino acids and sugars in the natural world. A combination of nonlinear effects and autocatalysis was first demonstrated experimentally by Soai to spontaneously generate asymmetry.[4] As derived by Kagan,[1] a nonlinear effect arises when one or more species in the system contain more than one unit of the chiral ligand, opening up the possibility of homochiral and heterochiral complexes. Depending on the system, there are several other conditions for a nonlinear effect, but one common feature is that the heterochiral complex must be more stable than its homochiral analogue. In favorable instances, direct spectroscopic observation of an equilibrium between homochiral and heterochiral complexes can establish a $\Delta\Delta G$, but such favorable conditions are not always available, and the measurement gives only relative, as opposed to absolute, thermochemical information. More usually, the relative stability of the diastereomeric complexes is inferred from molecular modeling, or simply guessed post facto. Given the multiple, subtle factors that can move $\Delta\Delta G$ by a few kcal/mol for or against the heterochiral complex, a priori predictions cannot be made with any claim of reliability. We report a gas-phase mass spectrometric study of 2:1 *bis*-oxazoline copper complexes in which the absolute ligand binding energies and the relative stabilities of the heterochiral and homochiral complexes are determined by energy-resolved collision-induced dissociation experiments. We compare the results to molecular modeling and make concrete predictions for nonlinear effects in copper-catalyzed cyclopropanation.

Experimental Section

Ligands **1**−**4** (Scheme 1), with and without labels, as well as their enantiomers, were synthesized according to literature procedures.[5,6] The syntheses and characterization are given in the Supporting Information. In a typical run, of which a specific instance for ligand **1** is representative, approximately 7 mg of the enantiomerically pure ligand (*S*,*S*)-**1a** are dissolved in 2.5 mL of dry CH_2Cl_2. A second stock solution of 7 mg of (*R*,*R*)-**1b** in 2.5 mL of CH_2Cl_2 is prepared similarly. A third stock solution is prepared by dilution of 2 mg (∼0.1 equiv relative to total *bis*-oxazoline) of tetrakis(acetonitrile)copper(I) hexafluorophosphate in 2.5 mL of dry CH_2Cl_2. The whole procedure is carried out in the glovebox.

(1) Kagan, H. B. *Adv. Synth. Catal.* **2001**, *343*, 227.
(2) Puchot, C.; Samuel, O.; Dunach, E.; Zhao, S.; Agami, C.; Kagan, H. B. *J. Am. Chem. Soc.* **1986**, *108*, 2253.
(3) Kitamura, M.; Okada, S.; Suga, S.; Noyori, R. *J. Am. Chem. Soc.* **1989**, *111*, 4028.
(4) Soai, K.; Shibata, T.; Sato, I. *Acc. Chem. Res.* **2000**, *33*, 382.
(5) Evans, D. A.; Woerpel, K. A.; Hinmann, M. M.; Faul, M. M. *J. Am. Chem. Soc.* **1991**, *113*, 726.
(6) Debono, N.; Besson, M.; Pinel, C.; Djakovitch, L. *Tetrahedron Lett.* **2004**, *45*, 2235. Werner, H.; Vicha, R.; Gissibl, A.; Reiser, O. *J. Org.Chem.* **2003**, *68*, 10166. Fraile, J. M.; Garcia, J. I.; Herrerias, C. I.; Mayoral, J. A.; Reiser, O.; Socuellamos, A.; Werner, H. *Chem.—Eur. J.* **2004**, *10*, 2997.

10.1021/ja065390p CCC: $37.00

Scheme 1

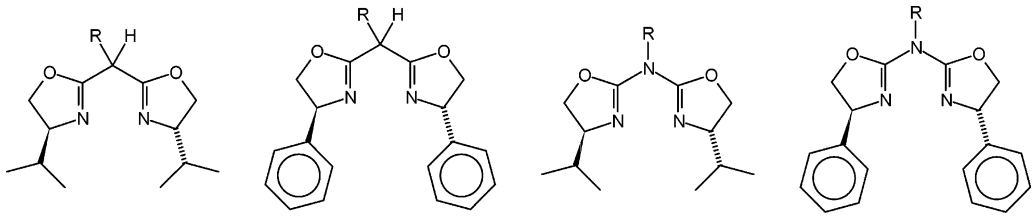

The 2:1 heterochiral complex was prepared in situ by combining 50 μL of each of the three stock solutions in a vial, which was stirred for 15 min at room temperature. The 2:1 homochiral complexes were prepared in situ by mixing 100 μL of either one of the ligand stock solutions with 50 μL of the copper(I) stock solution. The prepared solutions were stable for several days when kept at −37 °C in the freezer of the glovebox as evidenced by color and periodic checks by ESI-MS.

All measurements were performed on a Finnigan MAT TSQ-700 tandem mass spectrometer modified by replacement of the transfer octopole in the original triple quad instrument with a long radio frequency 24-pole ion guide. The 24-pole ion guide, 38 cm in length, can be run with a buffer or reagent gas at pressures up to 100 mTorr for thermalization or reaction without observable degradation of the ion current. No external longitudinal field is applied; ions move through the ion guide because of a weak longitudinal potential induced by the space charge from the continuous beam of incoming ions. In the present work, the principal significance of this modification is the achievement of a well-defined, narrow distribution of the ions' kinetic and, presumably, internal energies. These ions were thermalized to the 70 °C manifold temperature by collisions with 3 mTorr of buffer gas in the multipole and then mass-selected for CID in the first quadrupole of the TSQ-700. The selected ions were then injected into the octopole collision cell where they undergo CID with the target gas and subsequent mass analysis in the second quadrupole. The instrument has been described previously.[7] Instrument parameters are listed in the Supporting Information.

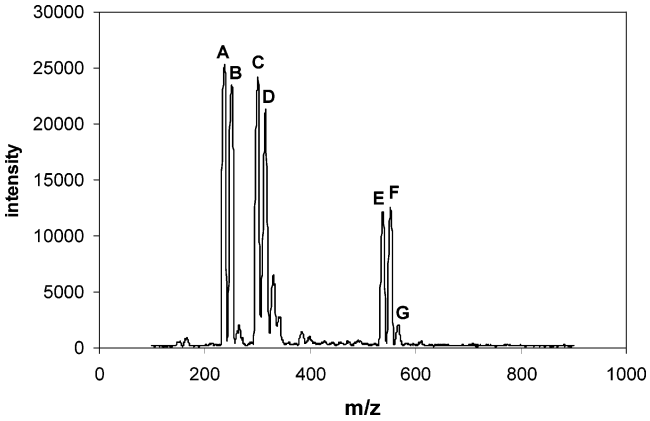

Figure 1. ESI-MS of the solution prepared from $Cu(CH_3CN)_4PF_6$, (*S*,*S*-**1a**) and (*R*,*R*-**1b**). The (*S*,*S*-**1a**)$_2$Cu$^+$ homochiral complex (m/z = 539, **E**), the (*S*,*S*-**1a**)(*R*,*R*-**1b**)Cu$^+$ heterochiral complex (m/z = 553, **F**), and the (*R*,*R*-**1b**)$_2$Cu$^+$ homochiral complex (m/z = 567, **G**), as well as the corresponding 1:1 complexes (m/z = 301, **C** and m/z = 315, **D**) and the free ligands (m/z = 238, **A**, and m/z = 252, **B**), appear in this mass spectrum. The ^{63}Cu/^{65}Cu splitting is not resolved.

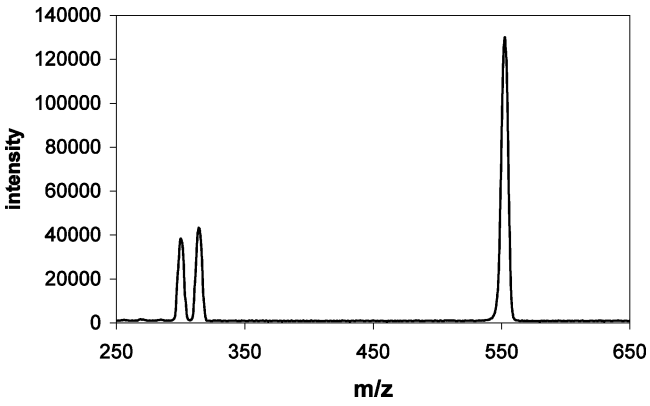

Figure 2. CID measurement of the (*S*,*S*-**1a**)(*R*,*R*-**1b**)Cu$^+$ heterochiral complex after mass selection of the parent, showing loss of either (*S*,*S*-**1a**) or (*R*,*R*-**1b**) (553 → 315 and 553 → 301).

Results

For spraying the copper−ligand solutions, approximately 10 μL of the prepared solution are diluted (in the glovebox) in 2.5 mL of dry CH_2Cl_2, which gives a final concentration of 13 μM, calculated per ligand. The electrospray mass spectrum clearly shows peaks corresponding to the 2:1 ligand−copper species, as well as 1:1 complexes and free ligand (visible as the protonated species). Given the absence of other ligands in the observed 1:1 complexes, they are probably daughter ions formed from the 2:1 complexes during the spray or desolvation process. For example, the solution with an in situ prepared heterochiral complex, shown in Figure 1, (*S*,*S*-**1a**)(*R*,*R*-**1b**)Cu$^+$, shows, apart from the expected 2:1 heterochiral complex, also the corresponding homochiral complexes, (*S*,*S*-**1a**)$_2$Cu$^+$ and (*R*,*R*-**1b**)$_2$Cu$^+$, with the relative peak intensities depending on the concentrations and relative stabilities of the various species in the particular example. The homochiral complexes, for example, (*S*,*S*-**1a**)$_2$Cu$^+$ and (*R*,*R*-**1b**)$_2$Cu$^+$ again, could also be generated independently, which was done in the cases where the equilibrium heavily favored the heterochiral complexes in solution.

Collision-induced dissociation (CID) of a mass-selected 2:1 complex proceeds with loss of one of the two *bis*-oxazoline ligands, as can be seen in the representative spectrum shown in Figure 2. No other products are observed, making the reaction ideal for modeling of the energy-resolved CID cross section. Importantly, complexes, such as (*S*,*S*-**1a**)(*R*,*R*-**1b**)Cu$^+$, which can lose either a labeled or unlabeled ligand, show both channels with nearly identical product intensity, indicating that the labeling itself has no large effect on the ligand binding energy in the best cases.

(7) Hammad, L. A.; Gerdes, G.; Chen, P. *Organometallics* **2005**, *24*, 1907.

Table 1. B3LYP/LANL2DZ Energies at DFT-Optimized Geometries for the Ions and Ligands

calculated substance	CID-measured substance	absolute energies in hartrees
(*R*,*R*-**1a**)$_2$Cu$^+$	(*S*,*S*-**1a**)$_2$Cu$^+$	−1732.953 641
(*R*,*R*-**1a**)(*S*,*S*-**1b**)Cu$^+$	(*S*,*S*-**1a**)(*R*,*R*-**1b**)Cu$^+$	−1772.267 293
(*R*,*R*-**1b**)$_2$Cu$^+$	(*R*,*R*-**1b**)$_2$Cu$^+$	−1811.564 599
(*R*,*R*-**1b**)Cu$^+$	(*R*,*R*-**1b**)Cu$^+$	−1003.762 153
(*R*,*R*-**1a**)Cu$^+$	(*S*,*S*-**1a**)Cu$^+$	−964.453 522
(*S*,*S*-**1b**)	(*R*,*R*-**1b**)	−807.746 19
(*S*,*S*-**1a**)	(*S*,*S*-**1a**)	−768.439 351
(*R*,*R*-**2a**)$_2$Cu$^+$	(*R*,*R*-**2a**)$_2$Cu$^+$	−2185.327 646
(*R*,*R*-**2a**)(*S*,*S*-**2b**)Cu$^+$	(*R*,*R*-**2a**)(*S*,*S*-**2b**)Cu$^+$	−2224.644 683
(*R*,*R*-**2b**)Cu$^+$	(*S*,*S*-**2b**)Cu$^+$	−1229.943 122
(*R*,*R*-**2a**)Cu$^+$	(*R*,*R*-**2a**)Cu$^+$	−1190.634 321
(*S*,*S*-**2b**)	(*S*,*S*-**2b**)	−1033.925763
(*S*,*S*-**2a**)	(*R*,*R*-**2a**)	−994.618 742
(*R*,*R*-**3b**)$_2$Cu$^+$	(*S*,*S*-**3b**)$_2$Cu$^+$	−1843.640 926
(*S*,*S*-**3b**)(*R*,*R*-**3c**)Cu$^+$	(*S*,*S*-**3b**)(*R*,*R*-**3c**)Cu$^+$	−1882.959 327
(*R*,*R*-**3c**)Cu$^+$	(*R*,*R*-**3c**)Cu$^+$	−1059.110 978
(*R*,*R*-**3b**)Cu$^+$	(*S*,*S*-**3b**)Cu$^+$	−1019.799 587
(*S*,*S*-**3c**)	(*R*,*R*-**3c**)	−863.085 13
(*S*,*S*-**3b**)	(*S*,*S*-**3b**)	−823.775 157
(*R*,*R*-**4a**)$_2$Cu$^+$	(*R*,*R*-**4a**)$_2$Cu$^+$	−2217.421 835
(*R*,*R*-**4a**)(*S*,*S*-**4b**)Cu$^+$	(*R*,*R*-**4a**)(*S*,*S*-**4b**)Cu$^+$	−2256.727 747
(*R*,*R*-**4b**)$_2$Cu$^+$	(*S*,*S*-**4b**)$_2$Cu$^+$	−2296.015 923
(*R*,*R*-**4a**)(*R*,*R*-**4b**)Cu$^+$	(*S*,*S*-**4a**)(*S*,*S*-**4b**)Cu$^+$	−2256.718 888
(*R*,*R*-**4b**)Cu$^+$	(*S*,*S*-**4b**)Cu$^+$	−1245.979 895
(*R*,*R*-**4a**)Cu$^+$	(*R*,*R*-**4a**)Cu$^+$, (*S*,*S*-**4a**)Cu$^+$	−1206.681 83
(*S*,*S*-**4b**)	(*S*,*S*-**4b**)	−1049.955 004
(*S*,*S*-**4a**)	(*S*,*S*-**4a**), (*R*,*R*-**4a**)	−1010.658 793

Retarding potential measurements for ions confirm that the modified instrument displays a close-to-Gaussian distribution of ion kinetic energies with a full width at half-maximum (fwhm) of 2.0−2.3 eV in the laboratory frame. The ion kinetic energy distribution showed no perceptible high-energy tail that would be otherwise present when the ion guide is of too low an order. The CID cross sections as a function of energy were measured for three to five different pressures of the xenon collision gas (between 30 and 120 μTorr) and extrapolated to zero pressure. Absolute cross sections, σ_p, were calculated as described by Ervin et al.[8] using a measured effective path length of 23 ± 5 cm. The uncertainty in the absolute cross sections is estimated to be ±50%.

Extraction of thermochemical information was performed with the CRUNCH program, version D1,[9] which fits the dissociation cross section σ to eq 1,

$$\sigma(E) = \left(\frac{n\sigma_0}{E}\right)\sum_i g_i \int_{E_0-E_i}^{E} [1 - \exp(-k(\epsilon + E_i)\tau)](E - \epsilon)^{n-1}\, d\epsilon \quad (1)$$

where E is the collision energy in the center-of-mass frame, E_0 is the reaction threshold energy at 0 K, σ_0 is a scaling factor, and n is an adjustable parameter. The summation is over i rovibrational states with energies E_i and populations g_i. The latter are assumed to follow a Maxwell−Boltzmann distribution at the temperature of the experiment. The parameter k is the RRKM dissociation rate for the ion with a residence time τ in the collision cell. The parameters σ_0, n, and E_0 are then optimized with a nonlinear least-squares analysis to give the best fit to the data. Equation 1 requires the frequencies for the complexes and transition states (to compute k), which were taken from quantum chemical calculations using Gaussian 03[10] running on AMD Athlon (small jobs), Athlon64, and Opteron (Red Hat EL 4 and Fedora Core 2 Linux) machines. The structures for the 2:1 complexes, as well as the dissociation products, were optimized with density functional theory (DFT) at the B3LYP/LANL2DZ level. The optimized structures were checked with frequency calculations to verify that they were in fact minima. The computed energies for the ligands and complexes in the experiment are listed in Table 1. The structures and frequencies for these complexes as well as the methyl- and ethyl-labeled analogues are given in the Supporting Information. Representative views of a pair of homo- versus heterochiral 2:1 complexes are shown in Figure 3. For all the CID thresholds, a loose orbiting transition state was assumed using the phase space limit model.[11] For collision-induced dissociations producing two products, the two-channel treatment with an additional scaling factor was used.[12] The density-of-states was computed using a Beyer−Swinehart direct state count within the harmonic oscillator approximation. Tests in which low frequency torsions were replaced with adiabatic free rotors showed no significant effect on the derived E_0.

It should be noted that the 2:1 complexes are sufficiently sterically constrained that even semiempirical methods, such as PM3, produce very similar structures. Furthermore, analogous Zn(II) complexes have been characterized crystallographically,

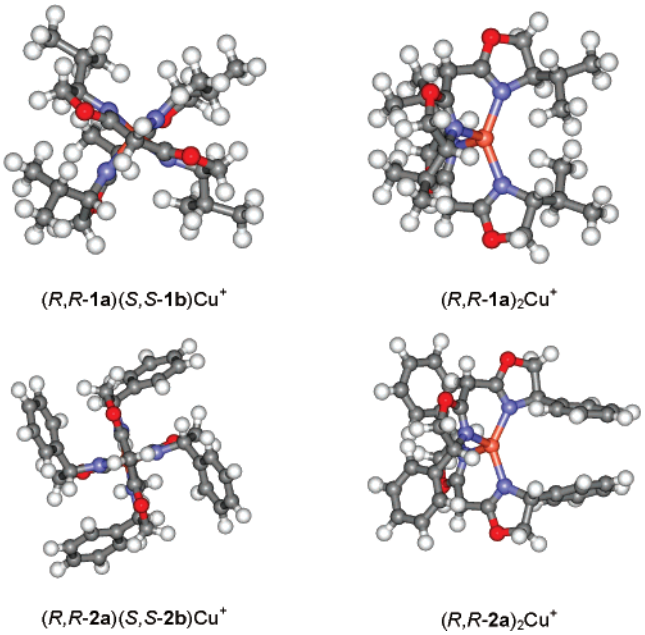

Figure 3. B3LYP/LANL2DZ-optimized geometries for (*R*,*R*-**1a**)(*S*,*S*-**1b**)Cu$^+$, (*R*,*R*-**1a**)$_2$Cu$^+$, (*R*,*R* -**2a**)(*S*,*S*-**2b**)Cu$^+$, and (*R*,*R*-**2a**)$_2$Cu$^+$.

(8) Ervin, K. M.; Armentrout, P. B. *J. Chem. Phys.* **1985**, *83*, 166. Schultz, R. H.; Crellin, K. C.; Armentrout, P. B. *J. Am. Chem. Soc.* **1991**, *113*, 8590. Dalleska, N. F.; Honma, K.; Sunderlin, L. S.; Armentrout, P. B. *J. Am. Chem. Soc.* **1994**, *116*, 3519.
(9) CRUNCH, version D1, was kindly provided as an executable by Prof. P. Armentrout.
(10) Frisch, et al. Gaussian 03, revision C.02; Gaussian, Inc.: Wallingford CT, 2004.
(11) Rodgers, M. T.; Ervin, K. M.; Armentrout, P. B. *J. Chem. Phys.* **1997**, *106*, 4499.
(12) Rodgers, M. T.; Armentrout, P. B. J. *Chem. Phys.* **1998**, *109*, 1787. Amicangelo, J. C.; Armentrout, P. B. *Int. J. Mass Spectrom.* **2001**, *212*, 301. Amicangelo, J. C.; Armentrout, P. B. *J. Phys. Chem. A* **2004**, *108*, 10698.

Table 2. Summary of Thermochemical Data from the Energy-Resolved Collision-Induced Dissociation Measurements and Comparison to DFT Predictions[a]

		single channel fit			two-channel fit			DFT calcd	
complex	ligand cleaved	E_0 (eV)	ΔS (eu)	ΔH (kcal/mol)	E_0 (eV)	ΔS (eu)	ΔH (kcal/mol)	ΔH (kcal/mol)	entry
(*S*,*S*-**1a**)$_2$Cu$^+$	(*S*,*S*-**1a**)	1.93	30	44.3				38.1	1
(*S*,*S*-**1a**)(*R*,*R*-**1b**)Cu$^+$	(*R*,*R*-**1b**)	2.05	26	47.2	2.05	26	47.2	42.2	2
(*S*,*S*-**1a**)(*R*,*R*-**1b**)Cu$^+$	(*S*,*S*-**1a**)	1.95	27	45.0	1.98	27	45.7	41.3	3
(*R*,*R*-**1b**)$_2$Cu$^+$	(*R*,*R*-**1b**)	1.84	24	41.9				35.3	4
labeling: H vs Me									
(*R*,*R*-**2a**)$_2$Cu$^+$	(*R*,*R*-**2a**)	2.21	33	50.7				46.8	5
(*R*,*R*-**2a**)(*S*,*S*-**2b**)Cu$^+$	(*S*,*S*-**2b**)	1.96	28	44.6	1.98	29	45.2	53.1	6
(*R*,*R*-**2a**)(*S*,*S*-**2b**)Cu$^+$	(*R*,*R*-**2a**)	1.97	27	44.9	2.01	27	45.9	52.0	7
labeling: H vs Me									
(*S*,*S*-**3b**)$_2$Cu$^+$	(*S*,*S*-**3b**)	2.06	25	47.0				41.5	8
(*S*,*S*-**3b**)(*R*,*R*-**3c**)Cu$^+$	(*R*,*R*-**3c**)	2.33	26	53.4	2.37	26	54.2	45.9	9
(*S*,*S*-**3b**)(*R*,*R*-**3c**)Cu$^+$	(*S*,*S*-**3b**)	2.27	25	52.0	2.31	25	52.8	46.8	10
labeling: Me vs Et									
(*R*,*R*-**4a**)$_2$Cu$^+$	(*R*,*R*-**4a**)	2.28	31	52.0				51.0	11
(*R*,*R*-**4a**)(*S*,*S*-**4b**)Cu$^+$	(*S*,*S*-**4b**)	2.28	24	51.9	2.43	24	55.4	57.0	12
(*R*,*R*-**4a**)(*S*,*S*-**4b**)Cu$^+$	(*R*,*R*-**4a**)	2.17	28	49.6	2.24	28	51.0	55.9	13
(*S*,*S*-**4b**)$_2$Cu$^+$	(*S*,*S*-**4b**)	2.07	31	47.3				50.8	14
(*S*,*S*-**4a**)(*S*,*S*-**4b**)Cu$^+$	(*S*,*S* -**4b**)	2.48	22	56.7	2.66	22	60.6	51.5	15
(*S*,*S*-**4a**)(*S*,*S*-**4b**)Cu$^+$	(*S*,*S*-**4a**)	2.19	27	50.0	2.23	27	50.8	50.3	16
labeling: H vs Me									

[a] The absolute uncertainties in E_0, ΔH, and ΔS are ±0.09 eV, ±2 kcal/mol, and ±0.03 eu, respectively.

and the structures are very similar.[13] The experimental energy-resolved dissociation cross sections could be fit either as single-channel events or, in the case of the heterochiral complexes, as two-channel processes. Fitting the individual channels of a two-channel process as single channels is not formally correct, but a glance at Table 2 shows that the differences are not large in a quantitative sense, and moreover, all qualitative trends remain unchanged. Presumably, the similar entropies of activations for the two channels make the energy dependences of the respective cross sections similar. Nevertheless, the quoted binding energies are given for the two-channel fits.

The ligand binding energies extracted from the experimental threshold curves are listed in Table 2, for which a representative data set, with the fit, is shown in Figure 4. Although the data quality is excellent, the assumptions built into the CRUNCH process introduce a certain range to the absolute ligand binding energies, E_0, typically cited to be 0.1 eV or, equivalently, about ± 2 kcal/mol. We performed control measurements, and data analysis under various assumptions, to establish the uncertainty bounds. As detailed in the Supporting Information, we find a global uncertainty of 0.08−0.09 eV, consistent with the usual bounds expressed in the literature. The structural similarity of all the compounds, however, should lead to cancelation of systematic errors, giving a much better relative accuracy. From the reproducibility of the curves and fittings, we estimate that the relative ligand binding energies, ΔE_0, to be better than ±1 kcal/mol. A necessary control for the cases of *pseudo*-racemates are the comparisons of the extracted thresholds for loss of differently labeled ligands, which are noted in Table 2.

Results for the 2:1 complexes with ligands **1** are given in entries 1−4 of Table 2. Comparing the loss of one ligand from each of the two homochiral complexes, (*S*,*S*-**1a**)$_2$Cu$^+$ and (*R*,*R*-**1b**)$_2$Cu$^+$, one finds similar thresholds, 44.3 and 41.9 kcal/mol, respectively. The heterochiral mixed complex (*S*,*S*-**1a**)(*R*,*R*-**1b**)Cu$^+$ loses either *S*,*S*-**1a** or *R*,*R*-**1b** upon CID with thresholds of 45.7 or 47.2 kcal/mol, respectively (Scheme 2). One sees first for the homochiral and then for the heterochiral complexes that the label R = H or CH_3 introduces only a small perturbation on the complexes. Second, the binding energy for the ligand to the heterochiral complex is significantly higher than the corresponding binding energy in the homochiral complexes. If one takes arithmetic means of the binding energies for the homo- versus heterochiral complexes, one finds that the heterochiral complex is more stable than the homochiral complex by 3.4 kcal/mol.

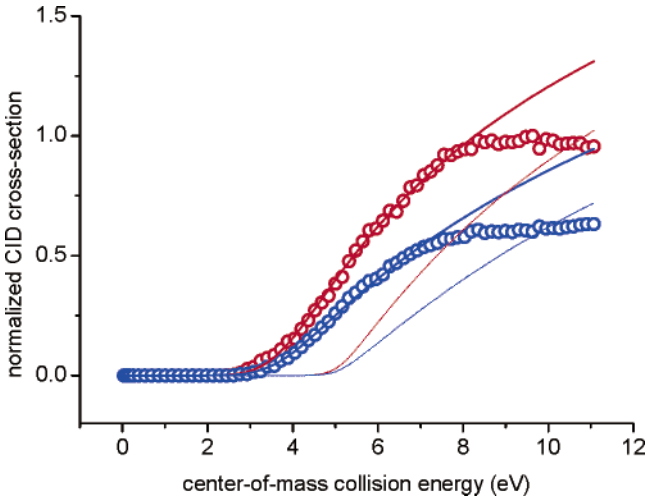

Figure 4. Two-channel fit for the collision-induced dissociation of (*S*,*S*-**1a**)(*R*,*R*-**1b**)Cu$^+$. The red data points and the heavy red fitted curve belong to the (*R*,*R*-**1b**)Cu$^+$ fragment, whereas the blue ensemble belongs to the (*S*,*S*-**1a**)Cu$^+$ fragment. The dotted lines show the unconvoluted thresholds.

Scheme 2

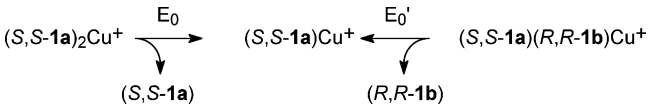

(13) Takacs, J. M.; Hrvatin, P. M.; Atkins, J. M.; Reddy, D. S.; Clark, J. L. *New J. Chem.* **2005**, *29*, 263.

For the azabox ligands with isopropyl substituents, **3**, the results for the dissociation of the 2:1 complexes are listed in entries 8−10 in Table 2. One would expect that the label of methyl versus ethyl for the azabox ligands would introduce a perturbation to the *pseudo*-enantiomers smaller than that in the hydrogen versus methyl pairs. In practice, both sets of labels produce acceptable control values, e.g., the heterochiral complex, (*S*,*S*-**3b**)(*R*,*R*-**3c**)Cu^+, shows for the loss of either *S*,*S*-**3b** or *R*,*R*-**3c** closely similar thresholds of 52.8 and 54.2 kcal/mol. The single measured homochiral complex (*S*,*S*-**3b**)$_2Cu^+$ shows for the loss of *S*,*S*-**3b** a much lower threshold of 47.0 kcal/mol. Again taking the mean for the heterochiral complex, the results indicate that the heterochiral complex is 6.5 kcal/mol more stable than the homochiral analogue.

Turning to the ligands, **2**, in which the oxazoline rings bear phenyl rather than isopropyl substituents, the situation changes, as seen in entries 5−7 in Table 2. The heterochiral complex, (*R*,*R*-**2a**)(*S*,*S*-**2b**)Cu^+, loses *R*,*R*-**2a** or *S*,*S*-**2b** with thresholds of 45.9 and 45.2 kcal/mol, respectively, even for the case of labels R = H versus CH_3. This indicates that the different labels in the *pseudo*-enantiomeric ligands really are innocuous for this complex. The homochiral complex, (*R*,*R*-**2a**)$_2Cu^+$, gives a much higher threshold of 50.7 kcal/mol. Taking the mean for the two thresholds from the heterochiral complex, the results indicate a reversal of stability, relative to the isopropyl-substituted cases, with the homochiral complex being more stable than its heterochiral relative by 5.1 kcal/mol when the oxazoline moiety carries a phenyl substituent.

The last combination of ligand backbone and oxazoline substituent, listed in entries 11−16 in Table 2, is the azabox ligand with phenyl substituents, **4**, which proved to be problematic. If the R = H or CH_3 labels were to behave innocuously, then both of the two homochiral combinations, (*R*,*R*-**4a**)$_2Cu^+$ and (*S*,*S*-**4b**)$_2Cu^+$, and the two channels for the heterochiral combination, (*R*,*R*-**4a**)(*S*,*S*-**4b**)Cu^+, would not show large deviations. However, (*R*,*R*-**4a**)$_2Cu^+$ shows a significantly higher threshold of 52.0 kcal/mol than does (*S*,*S*-**4b**)$_2Cu^+$, with 47.3 kcal/mol. Similarly unsatisfactory are the thresholds for the loss of *R*,*R*-**4a** versus *S*,*S*-**4b** from (*R*,*R*-**4a**)(*S*,*S* -**4b**)Cu^+, which, at 51.0 and 55.4 kcal/mol, are simply too far apart. Last, as a control experiment, a *pseudo*-homochiral complex, (*S*,*S*-**4a**)-(*S*,*S*-**4b**)Cu^+, dissociates by losing either *S*,*S*-**4a** or *S*,*S*-**4b**, two channels which should have the same, or very similar, thresholds. Experimentally, we find 50.8 and 60.6 kcal/mol, which means that the labels distinguishing *pseudo*-enantiomers exercise a strong influence on the stability of this 2:1 complex. In this case, the data cannot be used to judge the relative stability of homochiral versus heterochiral complexes. A pair of labels, such as R = C_2H_5 versus *n*-C_3H_7, would be expected to behave better, but these labels make the complex too large to be handled by CRUNCH.

Discussion

The experimental design required two choices: (*i*) choice of chemical system and (*ii*) choice of experimental technique. The *bis*-oxazoline ligands are readily available and, since their popularization by Evans,[5] have become one of the groups of "privileged structures" that appear repeatedly in asymmetric catalysis. Copper is an inexpensive metal whose catalytic chemistry spans a broad range of reactions in which the catalyst is usually generated in situ from metal salts and free ligands. Didactic models for asymmetric aldol and Diels−Alder reactions catalyzed by copper *bis*-oxazoline complexes assume 1:1 stoichiometry,[14] although there is little experimental evidence for or against the presumption. For many of the reactions, discrete intermediates and detailed mechanisms are not known; for example, the first isolated copper carbene complex[15] has been only recently reported despite a half-century's worth of catalytic cyclopropanation with copper salts, diazo compounds, and various additives.[16] Whereas the catalytically active copper complexes can be presumed to show a 1:1 stoichiometry with a *bis*-oxazoline ligand (if the complex is mononuclear), preliminary ESI-MS studies of CuOTf solutions with the *bis*-oxazoline ligands show that the 2:1 complex is the overwhelmingly predominant form and that ligand exchange is facile enough. Accordingly, the 2:1 complexes comprise an inactive reservoir from which the much less abundant active species are generated and to which active species can return. In the event that the *bis*-oxazoline ligand is enantiomerically impure, and if the heterochiral 2:1 complex were to be more stable than the homochiral one, then one can expect a positive nonlinear effect. The particular box and aza-box ligands used in this study, with isopropyl or phenyl substituents, are the most commonly used ligands in their family. Isopropyl and phenyl also show similar steric, but different electronic, properties, which permits a separation of these effects in the experiment.

Energy-resolved collision-induced dissociation cross-section measurements comprise a gas-phase, mass-spectrometric technique for the determination of binding energies of ligands to a metal ion.[17] The method has been applied extensively by Armentrout and others[18] to small-to-medium-sized ions. The work performed here explores the upper bound of size for ions that can be treated. CID thresholds directly address the relative stability of the hetero- vs homochiral complexes because the loss of one ligand from either 2:1 complex can produce the same 1:1 complex (or its enantiomer). Accordingly, the difference between the dissociation thresholds for the hetero- and homochiral complexes is exactly the difference in stability that is necessary (but not sufficient) for a nonlinear effect. Because mass spectrometry distinguishes ions according to the *m*/*z* ratio, *pseudo*-enantiomers of **1**−**4** were employed for this study. The long-established technique of substituting a remote site with a distinguishing label on two otherwise enantiomeric structures has been extensively used in pharmacological/metabolic studies[19] and has been more recently resurrected by Reetz[20] and by Pfalz[21] for the investigation of enantioselectivity in asymmetric

(14) Johnson, J. S.; Evans, D. A. *Acc. Chem. Res.* **2000**, *33*, 325.
(15) Straub, B. F.; Hofmann, P. *Angew. Chem.* **2001**, *113*, 1328.
(16) Kirmse, W. *Angew. Chem., Int. Ed.* **2003**, *42*, 1088.
(17) Ervin, K. M. *Chem. Rev.* **2001**, *101*, 391.
(18) Armentrout, P. B. *Thermochemical Measurements by Guided Ion Beam Mass Spectrometry;* Greenwich, CT, 1992; Vol. 1. Dalleska, N. F.; Honma, K.; Armentrout, P. B. *J. Am. Chem. Soc.* **1993**, *115*, 12125. Khan, F. A.; Clemmer, D. E.; Schultz, R. H.; Armentrout, P. B. *J. Phys. Chem.* **1993**, *97*, 7978. Poutsma, J. C.; Paulino, J. A.; Squires, R. R. *J. Phys. Chem. A* **1997**, *101*, 5336. Rodgers, M. T.; Armentrout, P. B. *J. Phys. Chem. A* **1997**, *101*, 1238. Hammad, L. A.; Wenthold, P. G. *J. Am. Chem. Soc.* **2000**, *122*, 11203. Hammad, L. A.; Wenthold, P. G. *J. Am. Chem. Soc.* **2001**, *123*, 12311.
(19) Jacques, J.; Collet, A.; Wilen, S. H. *Enantiomers, Racemates, and Resolutions*; Krieger Publishing Co.: Malabar, FL, 1994. Lettre, H.; Barnbeck, H.; Staunau, H. *Chem. Ber.* **1936**, *69b*, 1594.
(20) Reetz, M. T.; Becker,M. H.; Klein, H.-W.; Stöckigt, D. *Angew. Chem., Int. Ed.* **1999**, *38*, 1758.
(21) Markert, C.; Pfaltz, A. *Angew. Chem., Int. Ed.* **2004**, *43*, 2498.
(22) Bühl, M.; Kabrede, H. *J. Chem. Theory Comput.* **2006**, *2*, 1282.
(23) Sato, T.; Tsuneda, T.; Hirao, K. *J. Chem. Phys.* **2005**, *123*, 104307.

catalysis using mass spectrometry. In the present case, substitution at the backbone position of the *bis*-oxazolines **1**−**4** is presumed to exert only a small effect on their chemical properties, but the same substitution confers upon the *pseudo*-enantiomers distinguishable *m*/*z* ratios. In the best cases, labeling should be with methyl vs ethyl, or ethyl vs propyl, but even the a priori less ideal hydrogen vs methyl labels show a good internal consistency in the control experiments.

When consulting Table 2, several trends are evident. For the isopropyl-substituted ligands, **1** and **3**, the heterochiral 2:1 complex is more stable, with the difference, ΔE_0, between the (average) ligand binding energies of the hetero- vs homochiral complexes, increasing from 3.4 kcal/mol in the box ligands **1** to 6.5 kcal/mol in the azabox ligands **3**. The experimentally observed higher stability of the hetero- vs homochiral complex is readily explained on the basis of steric interactions if one looks at the computed geometry of the complexes in Figure 3. The homochiral complexes (*S*,*S*-**1a**)$_2$Cu$^+$ and (*S*,*S*-**3b**)$_2$Cu$^+$ are destabilized relative to the diastereomeric, hetereochiral complexes, (*S*,*S*-**1a**)(*R*,*R*-**1b**)Cu$^+$ and (*S*,*S*-**3b**)(*R*,*R*-**3c**)Cu$^+$, by unfavorable steric interactions of the isopropyl groups on the two ligands. Interestingly, the stability order is reversed for the complex with phenyl-substituted ligands, (*R*,*R*-**2a**)$_2$Cu$^+$ versus (*R*,*R*-**2a**)(*S*,*S*-**2b**)Cu$^+$, with the homochiral complex being in this case more stable. The comparable case for the complexes with phenyl-substituted azabox ligands, **4**, was uninformative in that the labels in the *pseudo*-enantiomers perturbed the system too much. Nevertheless, considering the complexes with ligands **2**, the homochiral 2:1 complex puts the phenyl groups in close proximity with each pair being oriented approximately parallel displaced, from which a stabilizing nonbonded interaction, e.g., dispersion, or more specifically, $\pi-\pi$ stacking, could come into play.

Interestingly, DFT calculations predict the heterochiral complex to be more stable than the homochiral for both the isopropyl and phenyl substituents. The computational level, DFT/LANL2DZ, is not particularly high, but it is representative of the current level one commonly finds for medium-to-large organometallic compounds in the literature. The steric crowding in the 2:1 complexes makes the level of theory less important for the gross geometry; there is no way for the phenyl or the isopropyl groups to avoid each other in the homochiral complexes. Whereas many studies have reported that DFT calculations reproduce geometries of organometallic complexes acceptably, the energies can be quite wrong.[22] In the present case, the DFT calculations underestimate ligand binding energies by up to 10 kcal/mol, but more importantly, they reverse the stability order for 2:1 complexes with phenyl-substituted ligands. Presumably, the discrepancy can be attributed to a known difficulty in DFT descriptions of long-range, nonbonded interactions, of which the interactions in the 2:1 homochiral complexes are a specific case. The magnitude of the discrepancy is surprisingly large, especially given that one is comparing stereoisomers. In a comparison of various DFT methods to CCSD(T) calculations for benzene dimers in various configurations, parallel face-to-face, T-shaped, and parallel displaced, the DFT methods, without corrections, missed attractive nonbonded minima identified by CCSD(T) calculations.[23] Uncorrected DFT calculations found purely repulsive potentials with absolute errors of ∼5 kcal/mol at CCSD(T)-detected energy minima. For the 2:1 complexes, there would be at least one such interaction, meaning that it is plausible that even the relative stability, homo- vs heterochiral, predicted by B3LYP/LANL2DZ could be wrong by at least 5 kcal/mol, which is consistent with our observed results.

If one considers the thermochemical results, it is clear that if a nonlinear effect of the simplest kind was to be explored with *bis*-oxazoline copper complexes as catalysts, the isopropyl-substituted ligands should display a nonlinear effect, but the sterically similar-sized phenyl-substituted ligands should not. Predictions based on DFT-computed stabilities would suggest that both isopropyl and phenyl substituents should give similarly large nonlinear effects. Moreover, the experimental observation that in situ preparation of 2:1 complexes by addition of copper salts and the free ligands to solution can produce variable results, depending on whether or not com- or disproportionation is fast enough to bring the mixture to thermodynamic equilibrium from the initially formed kinetically controlled composition. This observation suggests that, depending on the solvent and concentrations, nonlinear effects, or their absence, can be misleading unless the ligand−metal system has come to equilibrium before one initiates the catalytic reaction. Detailed solution-phase investigations are underway to check the prediction.

Conclusions

Quantitative energy-resolved collision-induced dissociation cross sections provide absolute thermochemical data for ligand binding to *bis*-oxazoline complexes of Cu(I). These complexes appear in catalysis and can show nonlinear effects, which should depend on the relative stability of homo- versus heterochiral 2:1 complexes. The measurements show that the heterochiral complexes are more stable when the oxazoline ring bears isopropyl substituents but that the stability order inverts when the substituent is phenyl. DFT calculations do not reproduce this stability order for the phenyl cases, but this can be attributed to DFT's difficulty in describing long range, nonbonded interactions.

Acknowledgment. The authors acknowledge support from the ETH Zürich and the Swiss Nationalfonds.

Supporting Information Available: Computed geometries, energies, for all of the complexes are listed. Reference mass spectra, as well as all of the energy-resolved collision-induced cross-section spectra, are also included. This material is available free of charge via the Internet at http://pubs.acs.org.

JA065390P